High Power Nitrogen-polar GaN/InAlN HEMT with Record Power Density of 12.8 W/mm at 28 GHz

S. Yoshida, K. Makiyama, A. Hayasaka, A. Mukai, I. Makabe, and K. Nakata

Transmission Devices Laboratory, Sumitomo Electric Industries, Ltd.
1, Taya-cho, Sakae-ku, Yokohama, Kanagawa, 244-8588, Japan
yoshida-shigeki1@sei.co.jp, +81-45-853-7318

Keywords: … HEMT, power amplifier, N-polar GaN, InAlN

Abstract

This paper describes the state-of-the-art large-signal performance of N-polar GaN/InAlN HEMT fabricated by the commercial 4-inch wafer process facilities. The N-polar GaN/InAlN HEMT epi-structure was grown on 4-inch semi-insulating SiC substrate by MOCVD. Hall measurement showed an electron mobility of 927.8 cm^2/Vsec, an electron density of 2.85×10^{13} cm^{-2}, and a sheet resistance of 236.4 Ω/sq with a low sheet resistance non-uniformity of 1.7%. The reported N-polar GaN/InAlN HEMT achieved a maximum drain current of 2.64 A/mm. S-parameter measurements revealed a current gain cutoff frequency of 30 GHz and a maximum oscillation frequency of 96 GHz. A saturated output power of 12.8 W/mm was achieved, and this was the highest output power for N-polar GaN HEMTs at Ka-band frequency. These results indicate that N-polar GaN/InAlN HEMT draws out the potential of N-polar GaN HEMT and paves the way for further high-power and high-frequency power amplifier.

INTRODUCTION

GaN HEMTs are currently indispensable for 4G and 5G systems. While gallium polar (Ga-polar) GaN devices have been widely used in the industry, a nitrogen polar (N-polar GaN) has attracted great interests. In particular, N-polar GaN HEMTs for RF power amplifiers have attracted considerable interest due to their potential for high power and high frequency characteristics [1-10]. Romanczyk et al. reported that output power (Pout) of 8.84 W/mm with power added efficiency (PAE) of 27.0% at 94 GHz [8]. Their results show that N-polar GaN HEMT significantly outperform Ga-polar GaN HEMT. Fabrication of N-polar GaN HEMT devices on 4-inch wafers has also been reported [11-13].

To further improve the output power and RF performance of Ga-polar GaN HEMTs, InAlN barriers have been adopted [14]. Specifically, $In_{0.17}Al_{0.83}N$ is lattice-matched to GaN and has higher polarization charge than that of AlGaN. N-polar InAlN HEMTs have also been reported to have similar advantages [15]. However, large signal characteristics of N-polar GaN/InAlN HEMTs have not yet been fully explored.

The objective of this study is to meet the demand of higher output power and higher frequency devices for high data-rate wireless communication networks. To this goal, we are focusing on N-polar GaN/InAlN HEMT. The device was designed to operate in the 28 GHz band, which has been allocated for 5G services. The device performances were evaluated by pulsed-IV, S-parameter, and load-pull measurements. The potential impact of this study is significant for developing N-polar GaN/InAlN HEMTs for high power and high frequency applications.

DESIGN AND FABRICATION OF THE DEVICE

N-polar GaN/InAlN HEMT epi-structure was grown on off-axis 4-inch semi-insulating SiC substrate by MOCVD. An InAlN back barrier was grown on the buffer layer. An AlN spacer, a 12-nm GaN channel and a cap layer were grown on the InAlN back barrier layer.

Following the epitaxial growth, gate insulators were deposited on the N-polar GaN/InAlN HEMT. The deposition process of $HfSiO_x$ for N-polar GaN HEMT was developed and it has relative permittivity of 13.5 and break down field of 8.5 MV/cm. Because of this high relative permittivity and break down field, $HfSiO_x$ was adopted to gate insulator.

n^+-GaN selective regrowth regions were introduced to reduce source and drain contact resistance. The designed gate length (L_g) was 200 nm, the source-drain length (L_{sd}) was 2.5 µm, the gate-source length (L_{gs}) was 0.9 µm, and the gate-drain length (L_{gd}) was 1.4 µm. The devices were fabricated using the same 4-inch wafer process facilities and on-wafer measurements were performed.

RESULTS AND DISCUSSIONS

Room temperature Hall measurement was performed. The measurement showed an electron mobility of 927.8 cm^2/Vs, an electron density of 2.85×10^{13} cm^{-2}, and a sheet resistance of 236.4 Ω/sq with a low sheet resistance non-uniformity of 1.7%.

Surface morphology of N-polar InAlN was compared to III-polar InAlN. Fig.1 shows AFM images (1 µm × 1 µm) of

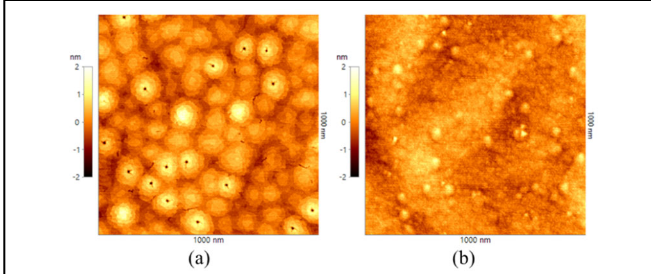

Fig. 1. AFM images (1 µm × 1 µm) of (a) III-polar and (b) N-polar InAlN.

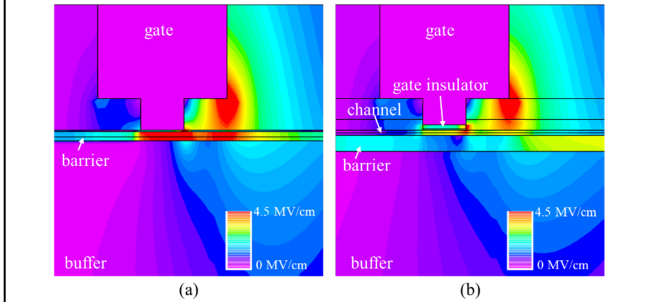

Fig. 2. Calculated electron field strength in (a) Ga-polar InAlN/GaN HEMT and (b) N-polar GaN/InAlN HEMT under off-state bias condition, V_g = -5 V and V_d = 50 V.

III-polar and N-polar InAlN. The root mean square roughness of III-polar InAlN was 0.379 nm, and that of N-polar InAlN was 0.304 nm. Compared to III-polar InAlN, the surface roughness of N-polar InAlN was smoother. This suppresses electron scattering and high electron mobility is expected. As shown in Fig. 1, small pits were observed on the surface of III-polar InAlN, and these pits can cause device breakdown and current collapse. On the other hand, such pits weren't observed on the surface of N-polar InAlN. Therefore, N-polar GaN/InAlN HEMT can be expected to have higher reliability and lower current collapse than Ga-polar.

The electric field strength inside the device was calculated using TCAD to design the device structure for high-voltage operation. Fig. 2 shows the simulated steady-state electric field strength in Ga- and N-polar GaN/InAlN HEMTs. The simulation was performed at off-state bias condition, V_g = -5 V and V_d = 50 V. As shown in Fig. 2, higher electric field strength is observed under the gate electrode in both devices. However, the strength was attenuated in N-polar GaN/InAlN HEMT. This can be explained as follows. In Ga-polar InAlN/GaN HEMT, external electric field by gate voltage is applied to InAlN barrier layer. In addition, internal electric field due to polarization of InAlN barrier layer is also applied and direction of the internal electric field is as same as the external electric field. Consequently, strong electric field is applied under a gate electrode. On the other hand, in N-polar GaN/InAlN HEMT, external electric field by gate voltage is applied to gate insulator and GaN channel layer. Polarization induced internal electric field of GaN is weaker than InAlN, and direction of the field is opposite to the external field. Therefore, the electric field under gate electrode in N-polar

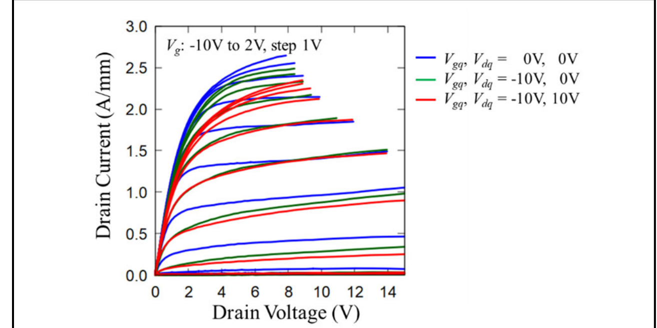

Fig. 3. Pulsed-IV characteristics with and without quiescent bias stresses.

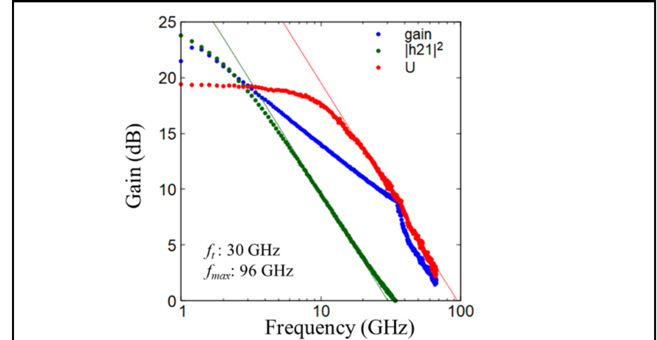

Fig. 4. The small signal RF characteristics. Slope of solid lines is -6 dB/oct.

GaN/InAlN HEMT is lower than Ga-polar InAlN/GaN HEMT. These simulation results indicate that N-polar GaN HEMTs have higher break down voltage and are more suitable for high voltage operation compared to Ga-polar GaN HEMTs.

The pulsed-IV measurements were performed with and without quiescent bias stresses. The quiescent condition was drain voltage (V_{gq} , V_{dq}) = (-10 V, 0 V) and (-10 V, 10 V). The results are shown in Fig. 3. The N-polar GaN/InAlN HEMT achieved a maximum drain current density of 2.64 A/mm without quiescent bias stress. As shown in Fig. 3., low current collapse is observed with quiescent bias stresses. The drain current of the N-polar GaN/InAlN HEMT was decreased by 4.1% and 14.5% at V_{ds} = 5 V and gate voltage V_{gs} = 2 V after the quiescent bias stresses, (-10 V, 0 V) and (-10 V, 10 V), were applied.

S-parameter measurements were performed at V_{ds} = 15 V, I_{ds} ~ 600 mA/mm. The results are shown in Fig. 4. The maximum stable gain of the N-polar GaN/InAlN HEMT was 10.5 dB at 28 GHz. A current gain cutoff frequency f_t = 30 GHz and a maximum frequency of oscillation f_{max} = 96 GHz were extracted by extrapolating current gain ($|h_{21}|^2$) and a unilateral gain (U).

Load-pull measurements at 28 GHz were performed on the N-polar GaN/InAlN HEMT and the device was biased in class AB with V_{dq} = 28 V and I_{dq} = 250 mA/mm. Those measurements were on-wafer measurements without pre-matching circuits. We note that impedance tuning range was limited during the load pull measurements.

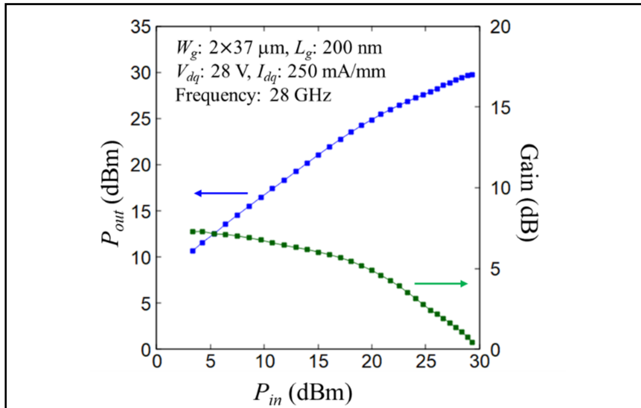

Fig. 5. 28-GHz load-pull power sweeps with the device biased at V_{dsq} = 28 V and I_{dsq} = 250 mA/mm.

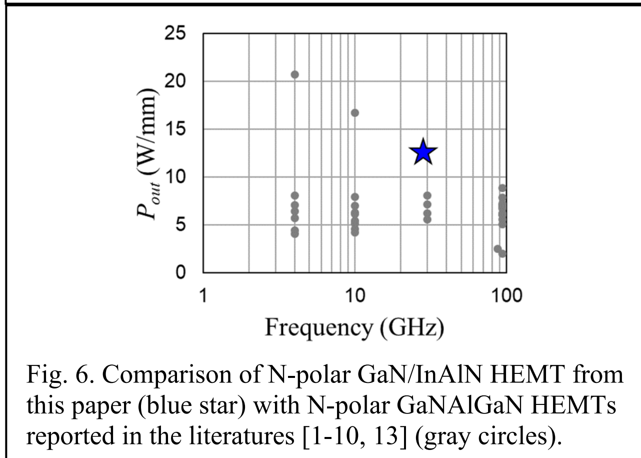

Fig. 6. Comparison of N-polar GaN/InAlN HEMT from this paper (blue star) with N-polar GaNAlGaN HEMTs reported in the literatures [1-10, 13] (gray circles).

Because the optimal gammas were greater than the available tuning range, the device output power and gain of the device are limited. As shown in Fig. 5, the device exhibited a saturated output power (P_{sat}) of 12.8 W/mm (29.8 dBm) which is the best reported power performance for N-polar GaN HEMTs at Ka-band frequency as shown in Fig. 6. Considering the limitation of impedance tuning, N-polar GaN/InAlN HEMT has potential to exhibit higher output power. These results indicate that N-polar GaN/InAlN HEMT draws out the potential of N-polar GaN HEMT and paves the way for further high-power and high-frequency power amplifiers.

Conclusions

We reported the large-signal performance of N-polar GaN/InAlN HEMT for high power and high-frequency power amplifier applications. The smooth surface of N-polar InAlN increases break down field and improves reliability. The N-polar GaN/InAlN HEMT achieved a maximum drain current of 2.64 A/mm and a saturated output power of 12.8 W/mm, which was the highest output power for N-polar GaN HEMT at Ka-band frequency. These results suggest that N-polar GaN/InAlN HEMT has great potential for further high-power and high-frequency power amplifier.

Acknowledgements

This work is based on results obtained from "Research and Development Project of the Enhanced Infrastructure for Post-5G Information and Communication System" JPNP20017, subsidized by the New Energy and Industrial Technology Development Organization (NEDO).

References

[1] U. K. Mishra et al., *N-polar GaN-based MIS-HEMTs for mixed signal applications*, 2010 IEEE MTT-S International Microwave Symposium, pp. 1130-1133, 2010.
[2] S. Kolluri, et al., IEEE Electron Device Lett., **33**, 44 (2012).
[3] X. Zheng et al., *High frequency N-polar GaN planar MIS-HEMTs on sapphire with high breakdown and low dispersion*, 2016 Lester Eastman Conference (LEC), Bethlehem, pp. 42-45, 2016.
[4] X. Zheng et al., IEEE Electron Device Lett., **37**, 77 (2016).
[5] B. Romanczyk et al., Electron. Lett., **52**, 1813 (2016).
[6] S. Wienecke et al., IEEE Electron Device Lett., **38**, 359 (2017).
[7] B. Romanczyk et al., IEEE Trans. Electron Devices, **65**, 45 (2018).
[8] B. Romanczyk et al., IEEE Electron Device Lett., **41**, 349 (2020).
[9] W. Liu et al., IEEE Microw. Wirel. Compon. Lett., **31**, 748 (2021).
[10] E. Akso et al., IEEE Microw. Wirel. Technol. Lett., **33**, 683 (2023).
[11] D. Bisi et al., *Commercially Available N-polar GaN HEMT Epitaxy for RF Applications*, 2021 IEEE 8th Workshop on Wide Bandgap Power Devices and Applications (WiPDA), pp. 250-254, 2021.
[12] S. Yoshida et al., *Challenges and Potential of N-polar GaN HEMT for beyond 5G Wireless Network*, 2022 IEEE BiCMOS and Compound Semiconductor Integrated Circuits and Technology Symposium (BCICTS), pp. 104-107, 2022.
[13] A. Arias-Purdue et al., IEEE Microw. Wirel. Technol. Lett., **33**, 1011 (2023).
[14] K. Makiyama et al., *Collapse-free high power InAlGaN/GaN-HEMT with 3 W/mm at 96 GHz*, 2015 IEEE International Electron Devices Meeting (IEDM), pp. 9.1.1-9.1.4, 2015.
[15] D. Denninghoff, et al., *N-polar GaN/InAlN/AlGaN MIS-HEMTs with 1.89 S/mm extrinsic transconductance, 4 A/mm drain current, 204 GHz fT and 405 GHz fmax,* 71st Device Research Conference, pp. 197-198, 2013.

Acronyms

HEMT: High Electron Mobility Transistor
MOCVD: Metal Organic Chemical Vapor Deposition